Preprints of the 21st IFAC World Congress (Virtual)
Berlin, Germany, July 12-17, 2020

PK/PD-Based Impulsive Control to Tailor Therapies in Infectious Diseases ⋆

Gustavo Hernandez-Mejia [*,***]
Esteban A. Hernandez-Vargas [**,*]

[*] *Frankfurt Institute for Advanced Studies, Frankfurt am Main, Germany*
[**] *Instituto de Matematicas, UNAM, Unidad Juriquilla, Mexico*
[***] *Faculty of Biological Sciences, Goethe University, Frankfurt am Main, Germany*

Abstract: Strategic initiatives in pharmaceutical companies and drug research have incorporated the pharmacokinetics (PK) and pharmacodynamics (PD) modeling, known as the PK/PD framework. Herein, we use an inverse optimal impulsive approach to devise PK/PD-based treatment policies for infectious diseases such as HIV and influenza. The optimal PK/PD-based HIV therapy maintains the viral load under detection levels for a thirty-year period when the treatment initiates 2 or 4 years post-infection. We also explore the implications of late HIV treatment initiation. On the other hand, the optimal PK/PD-based influenza treatment reduces ca. 30% the amount of drug compared to the treatment recommended by the Food and Drug Administration while reaching the same efficacy levels (98%). The PK/PD framework mastermind new schemes for tailoring treatments in infectious diseases.

Keywords: PK/PD Dynamics, Biomedical Systems, Impulsive Control, Influenza, HIV.

1. INTRODUCTION

Infectious diseases are a great threat to humanity. HIV-related illnesses and deaths, for instance, have resulted in more than 32 million fatalities. At the global level, in 2018 the number of HIV-related mortal cases reached 770 000 [WHO (2019-Online)]. Also worldwide, outbreaks caused by influenza A viruses (IAV) have annually revealed high morbidity and mortality. The IAV threat results in about 500,000 deaths and up to 5 million severe cases [WHO (2018-Online)]. Three phases can be identified during HIV infection response, an initial acute infection followed by a long asymptomatic period and, finally, a vast increment of viral load with the simultaneous downfall of healthy CD4+ T cell [Hernandez-Vargas and Middleton (2013)]. For HIV, the combined antiretroviral treatment (cART) leads the virus to undetectable levels and guard against the harm of other infections [HIV-CC (2010)]. The current Food and Drug Administration (FDA) approved IAV treatment uses fixed doses of neuraminidase inhibitors (NI) twice a day.

Drug development and design demand the understanding of mechanisms of drug delivery and response. The pharmacologic disciplines, pharmacokinetics (PK) and pharmacodynamics (PD), coupled as the PK/PD approach, benefit from diverse preclinical and clinical data using mathematical frameworks, leading to guide decision-making through modeling and simulation [Yu et al. (2019)]. The PK/PD framework also boost the researchers understanding of drug behavior and effectiveness at individual and demographic levels [Gabrielsson and Weiner (2017)]. Drug optimization is supported by PK/PD models at all development stages, allowing pharmaceutical companies to improve efficacy and productivity [Van der Graaf and Benson (2011)]. Importantly, for the case of HIV and influenza therapies, PK/PD drug parameters are available.

Based on mathematical models of biological systems, recent theoretical impulsive control approaches have been integrated to design treatment schedules for diabetes [González et al. (2017)] and infectious diseases such as HIV [Zurakowski and Teel (2006); Rivadeneira et al. (2017)] and IAV [Hernandez-Mejia et al. (2019)]. The impulsive control scheme deals with systems in which at least one state can be impulsively changed at certain control instants [Yang (2001)]. Besides, the effort of the impulsive state modification can be governed by optimal control techniques ensuring stability under an optimality criterion [Hernandez-Mejia et al. (2019)]. In this sense, the inverse optimal control framework sets a control law and then an optimal criterion is derived [Haddad et al. (2006)].

Herein, we integrate a control-based framework accounting for inverse optimal impulsive control strategies to design treatment schedules based on the viral dynamics and the drug's PK/PD phases. We envisage PK/PD-based treatments for both, cART and oseltamivir, in HIV and IAV infectious diseases. While for cART treatment we hypothesize a scheme under unified PK/PD parameters, the oseltamivir treatment integrates its nominal values. The PK/PD-based control treatment is tested with different treatment initiation time in HIV, fixed time in IAV, and a maximum intake drug amount in each treatment.

⋆ We thank the supported of the Alfons und Gertrud Kassel-Stiftung and the Deutsche Forschungsgemeinschaft through the project HE7707/5-1. Corresponding author: esteban@im.unam.mx

2. INVERSE OPTIMAL IMPULSIVE CONTROL

Notation. $\Re$ is the set of real numbers, $\Re^{n\times m}$ is the set of $n \times m$ real matrices and $\Re^n$ is the set of $n \times 1$ column vectors. $\aleph = \mathbb{Z}^+ \cup \{0\}$ is the set of non-negative integers and $S \subset \aleph$ is the resetting set for control instants action. The set of $n\times n$ positive-definite matrices is P^n, the matrix transpose is $(\cdot)^T$, the diagonal matrix given by $\text{diag}(\cdot)$ and the matrix inverse is $(\cdot)^{-1}$.

The impulsively controlled system has the form

$$\dot{x}(t) = f(x(t)),\ x_0 = x(0),\ t \neq \tau_j, \tag{1}$$

$$\Delta x(t) = f(x(\tau_j)) + g(x(\tau_j))\,\text{sat}(u(\tau_j)),\ t = \tau_j, \tag{2}$$

$$\text{sat}(u(\tau_j)) = \min\big(u(\tau_j), u_{max}(\tau_j)\big), \tag{3}$$

where $\tau_j \in S$ are the impulsive control instants. $x(\tau_j) \in \Re^n$ is the state at τ_j, $x(t) \in \Re^n$ is the state of the system in $t \neq \tau_j$. The input $u(\tau_j) \in \Re^m$, and functions $f : \Re^n \to \Re^n$, $g : \Re^n \to \Re^{n\times m}$. $\Delta x(t)$ stands for the impulsive state modification at the control instant τ_j. The impulsive changes modify the initial condition for the following integration step with an instantaneous jump as follows

$$x(\tau_j^+) = \ \Delta x(t)\big|_{t=\tau_j} + x(\tau_j^-), \tag{4}$$

$$\dot{x}(t) = f(x(\tau_j^+)), \quad t = \tau_j, \tag{5}$$

where $x(\tau_j^+)$ is the newly generated initial condition due to the impulsive change and $x(\tau_j^-)$ is the state before the impulsive jump. For the state modification with the impulsive law in (2), from the optimal control theory [Haddad et al. (2006); Hernandez-Mejia et al. (2018)], we follow to minimize the cost functional

$$Q(x(\tau_j)) = \sum_{\tau_j \in S}^{\infty} \big(l(x(\tau_j)) + u(\tau_j)^T R u(\tau_j)\big), \tag{6}$$

where $Q : \Re^n \to \Re^+$, $l : \Re^n \to \Re^+$ weights the state vector $x(\tau_j)$ and is positive semidefinite. Besides, $R : \Re^n \to P^m$ weights the control effort.

Consider the impulsively controlled system (2) and, for simpler notation, $x(\tau_j^+)$ standing for the state change in the impulsive instant, we use the following optimal control law [Hernandez-Mejia et al. (2018); Sanchez and Ornelas-Tellez (2017)]

$$u(\tau_j)^* = -\frac{1}{2} R^{-1} g(x(\tau_j))^T \frac{\partial Q^*(x(\tau_j^+))}{\partial(x(\tau_j^+)),} \tag{7}$$

which is inverse optimal if satisfies the following; 1) it achieves exponential stability of the equilibrium point $x(\tau_j) = 0$ for system (2) (globally) with the optimal value function $Q^*(x(0)) = Q(x(0))$, 2) it satisfies the cost functional (6), accounting for $l(x(\tau_j)) := -\overline{Q}$ and

$$\overline{Q} := u(\tau_j)^{*T} R u(\tau_j)^* + Q(x(\tau_j^+)) - Q(x(\tau_j)) \leqslant 0. \tag{8}$$

Next, it follows that a function $Q(x(\tau_j))$ can be designed to satisfy (7)-(8). In this direction, we consider $Q(x(\tau_j))$ in the following form [Sanchez and Ornelas-Tellez (2017)]

$$Q(x(\tau_j)) = \frac{1}{2} x(\tau_j)^T P_j x(\tau_j),\ P_j = P_j^T > 0, \tag{9}$$

which is used in the optimal control law (7) selecting a proper matrix $P_j \in P^n$. The inverse optimal impulsive control law is obtained applying (9) to (7) and optimizes the cost functional (6). Control law (7) is then modified to integrate the inverse approach as follows

$$\begin{aligned} u(\tau_j)^* &= -\frac{1}{2} R^{-1} g(x(\tau_j))^T \frac{\partial Q^*(x(\tau_j^+))}{\partial(x(\tau_j^+))}, \\ &= -\frac{1}{2} R^{-1} g(x(\tau_j))^T \frac{\partial\Big(\frac{1}{2} x(\tau_j^+)^T P_j x(\tau_j^+)\Big)}{\partial(x(\tau_j^+))}, \\ &= -\frac{1}{2} R^{-1} g(x(\tau_j))^T P_j \Big(x(\tau_j) + f(x(\tau_j))\Big) \\ &\quad -\frac{1}{2} R^{-1} g(x(\tau_j))^T P_j g(x(\tau_j)) u(\tau_j)^*. \end{aligned} \tag{10}$$

From (10), it follows solving for $u(\tau_j)^*$

$$\begin{aligned} &u(\tau_j)^* + \frac{1}{2} R^{-1} g(x(\tau_j))^T P_j g(x(\tau_j)) u(\tau_j)^* \\ &= -\frac{1}{2} R^{-1} g(x(\tau_j))^T P_j \big(x(\tau_j) + f(x(\tau_j))\big), \end{aligned} \tag{11}$$

multiplying (11) by R, it follows

$$\begin{aligned} &(R + \frac{1}{2} g(x(\tau_j))^T P_j g(x(\tau_j))) u(\tau_j)^* \\ &= -\frac{1}{2} g(x(\tau_j))^T P_j \big(x(\tau_j) + f(x(\tau_j))\big). \end{aligned} \tag{12}$$

Finally, from (12), the inverse optimal impulsive control law $u(\tau_j)^*$ can be expressed as

$$u(\tau_j) = -\frac{1}{2}\big(R + P_\alpha(x(\tau_j))\big)^{-1} P_\beta(x(\tau_j)), \tag{13}$$

$$P_\alpha(x(\tau_j)) = \frac{1}{2} g(x(\tau_j))^T P_j g(x(\tau_j)),$$

$$P_\beta(x(\tau_j)) = g(x(\tau_j))^T P_j \big(x(\tau_j) + f(x(\tau_j))\big).$$

Importantly, inverse matrix form in (13) is satisfied since $P_\alpha(x(\tau_j)$ is a symmetric and positive definite matrix [Hernandez-Mejia et al. (2018); Sanchez and Ornelas-Tellez (2017)].

The constraining input, $\text{sat}(u(\tau_j))$, considers the maximum value $u_{max}(\tau_j)$ in (3), this is incorporated in terms of R in (13) as follows

$$\begin{aligned} 2u(\tau_j) &= -\big(R + P_\alpha(x(\tau_j))\big)^{-1} P_\beta(x(\tau_j)), \\ 2\big(R + P_\alpha(x(\tau_j))\big) u(\tau_j) &= -P_\beta(x(\tau_j)), \\ 2Ru(\tau_j) &= -P_\beta(x(\tau_j)) \\ &\quad -2P_\alpha(x(\tau_j)) u(\tau_j). \end{aligned} \tag{14}$$

For a given u_{max}, the value of R in (14) is given by

$$R = -\frac{1}{2}\left[\frac{P_\beta(x(\tau_j)) + 2P_\alpha(x(\tau_j)) u_{max}}{u_{max}}\right]. \tag{15}$$

Usually, the value of u_{max} is a priori given as, for instance, the maximum quantity of effort that the controller can handle due to physical or design limitations.

3. PK/PD-BASED TREATMENT FORMULATION

The PK/PD-based control framework allows conceiving a control law whose structure incorporates the viral dynamics (or any other affine system) and PK/PD effects. As shown in Fig. 1, whenever $t \neq \tau_j$ (solid arrow) the viral and PK/PD dynamics behave as at open loop, however, when $t = \tau_j$ (dotted arrows), at least one of the states of the PK/PD-system is impulsively modified following (4), where the control effort is given by (13). In addition, using dynamic values of R in (15), the value of u_{max} considers dose constraints as, for instance, the maximum quantity of dose for a single intake. Finally, the drug intake frequency is no other than the impulsive instants, in other words, τ_j stands for the drug intake time (usually in hours).

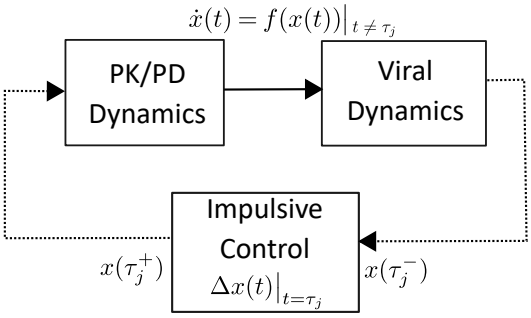

Fig. 1. **Scheme of the PK/PD-based impulsive control**. Whenever $t \neq \tau_j$, the viral and PK/PD dynamics behave as at open-loop (solid arrow). The impulsive control modifies the PK/PD-state of the system at $t = \tau_j$, which changes from $x(\tau_j^-)$ to $x(\tau_j^+)$ (dotted arrows), which corresponds with the drug dose.

Importantly, the PK/PD dynamics module in Fig. 1 is integrated by the PK and PD phases, where the PK phase is commonly constructed by at least one differential equation (compartment) describing the amount of available drug and its elimination rate. However, the PK phase can contain as many compartments as necessary to describe the drug distribution in organs and drug decomposition. The PD phase has a direct effect on the viral dynamics by means of the drug efficacy which is usually given by the EC_{50} value, which is the drug concentration level at which provides the 50% of drug efficacy. On the other hand, the viral dynamics module integrates diverse host dynamics that are important for the study of the infection and the treatment. In this framework, the PK/PD-based control compute the quantity of drug accounting for the drug compartments, drug efficacy, drug intake frequency, and host-related dynamics.

4. PK/PD-BASED HIV TREATMENT

4.1 HIV and drug dynamics

Recent clinical observations contemplate that the early initiation of cART is central for the gradual and successful contraction of the HIV reservoir (shrink), which must be eventually depleted. These therapeutic strategies focus on kicking (activate) the latent reservoir and reinforcing the clearance (kill) of virus-infected cells, this scheme is known as the "kick-kill" strategy [Hernandez-Vargas (2017)]. In this sense, the time window for the effective performance of a "shrink-kick-kill" strategy, while the early phase of the infection shows limited reservoirs, is narrow but decisive, see Fig. 2.

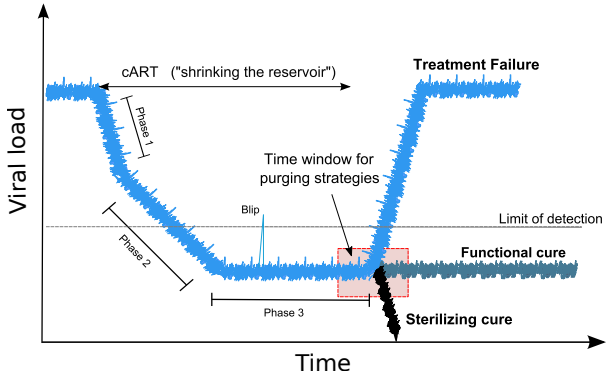

Fig. 2. **Treatment strategies for HIV.** cART drives to a sterilizing or a functional cure by managing a controlled viremia below the limit of detection [Hernandez-Vargas (2017)].

The model herein employed considers the infected and healthy (uninfected) active CD4+ T cells, given by T_i and T, respectively. It also incorporates the infected and uninfected macrophages, M_i and M, respectively, and the HIV, V. The model writes as follows [Hernandez-Vargas and Middleton (2013)]:

$$\dot{T}(t) = s_1 + \frac{p_1}{V(t)+C_1}T(t)V(t)\left(1 - \frac{D(t)}{D(t)+EC_{50}}\right) - \delta_1 T(t) - k_1 T(t)V(t), \quad (16)$$

$$\dot{T}_i(t) = k_1 T(t)V(t)\left(1 - \frac{D(t)}{D(t)+EC_{50}}\right) - \delta_2 T_i(t), \quad (17)$$

$$\dot{M}(t) = s_2 + \frac{p_2}{V(t)+C_2}V(t)M(t) - \delta_3 M(t) - k_2 M(t)V(t), \quad (18)$$

$$\dot{M}_i(t) = k_2 M(t)V(t) - \delta_4 M_i(t), \quad (19)$$

$$\dot{V}(t) = k_3 T_i(t)\left(1 - \frac{D(t)}{D(t)+EC_{50}}\right) + k_4 M_i(t) - \delta_5 V(t), \quad (20)$$

$$\dot{D}(t) = -\delta_D D(t), \ t \neq \tau_j, \ \tau_j \leqslant t < \tau_{j+1} \quad (21)$$

$$D(\tau_j^+) = U_D(\tau_j) + D(\tau_j^-), \ t = \tau_j. \quad (22)$$

The CD4+ T cells and macrophages growth rates are p_1 (0.01 day^{-1}) and p_2 (0.003 day^{-1}), respectively, with carrying capacities C_1 (300 copies/mm^3) and C_2 (220 copies/mm^3), respectively. Free virus infects CD4+ T cells at rate k_3 (4.57×10^{-5} mm^3/day copies). CD4+ T cells die at rate δ_1 (0.01 day^{-1}). The new cell source terms are s_1 (10 cells/mm^{3}day) and s_2 (0.15 cells/mm^{3}day). The clearance of infected CD4+ T cells is δ_2 (0.4 day^{-1}). The free virus infects macrophages at rate k_2 (4.33×10^{-8} mm^3/day copies). M_i and M die at rate δ_4 (1×10^{-3} day^{-1}) and δ_3 (1×10^{-3} day^{-1}), respectively. Furthermore, infected CD4+ T cells and macrophages produce virus at rates k_3 (38 copies/cell day) and k_4 (35 copies/cell

day), respectively. The clearance of virions (viral particles) is δ_5 (2.4 day^{-1}). δ_5 (2.4 day^{-1}) is the clearance of viral particles. CD4+ T cells initiates as 1000 cells/mm^3 and macrophages as 150 cells/mm^3, the infected cells are initiated zero and the initial viral load as 10 copies/ml [Hernandez-Vargas and Middleton (2013)]. For drug effects, the PK phase is modeled by the constant decay compartment (21) considering the drug amount available (D) and the rate of drug elimination δ_D (1.5 days^{-1}). The PD phase considers the EC_{50} (42 mg) parameter. The drug intake fixed time is given by τ_j, where $j = 24 \times 1, 2, \cdots$, which guides the sequence of drug intakes, in this case, each 24 h. The HIV system (16)-(21) does not consider the mutation process of HIV and the action of different drugs in the treatment, however, we investigate the treatment tailoring using a unified efficacy framework of HIV drugs and the adaptive scheme of drug dose under PK/PD control-based tailoring.

4.2 PK/PD-based HIV treatment

For the impulsive control law (13) in HIV treatment, we consider matrix $P_{j(HIV)} = \text{diag}(1000)$ and $u_{max} = 1000$ mg as the maximum drug dose per intake. We further use the absolute value of the control law and matrix R to produce only positive values of drug amounts. The state vector form is $x(t) = [T(t), T_i(t), M(t), M_i(t), V(t), D(t)]$ and $g(x(\tau_j)) = [0, 0, 0, 0, 0, 1]$ to form matrices $P_\alpha(x(\tau_j))$ and $P_\beta(x(\tau_j))$ of control law (13).

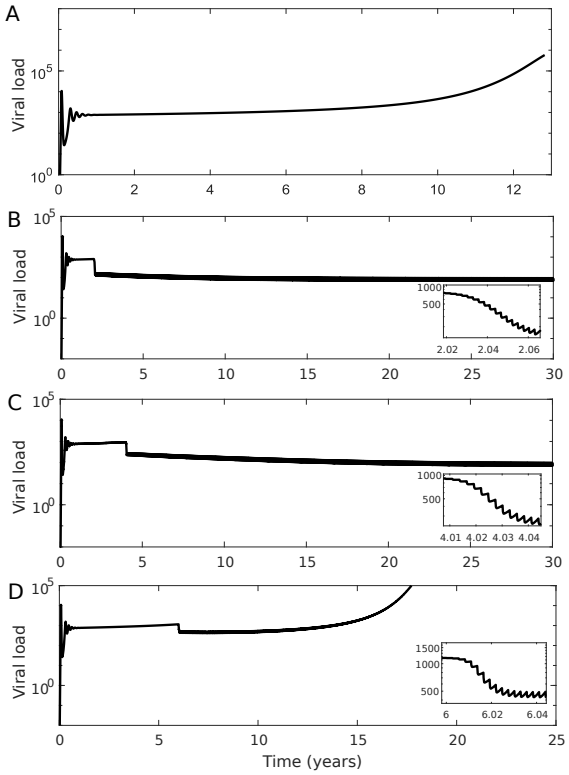

Fig. 3. **Effects of PK/PD-based control treatment in HIV viral load**. A) case without treatment, B-D) depict treatments initiated at 2, 4 and 6 ypi, respectively. Zoom windows allow identifying the viral impulsive elimination from the treatment initiation.

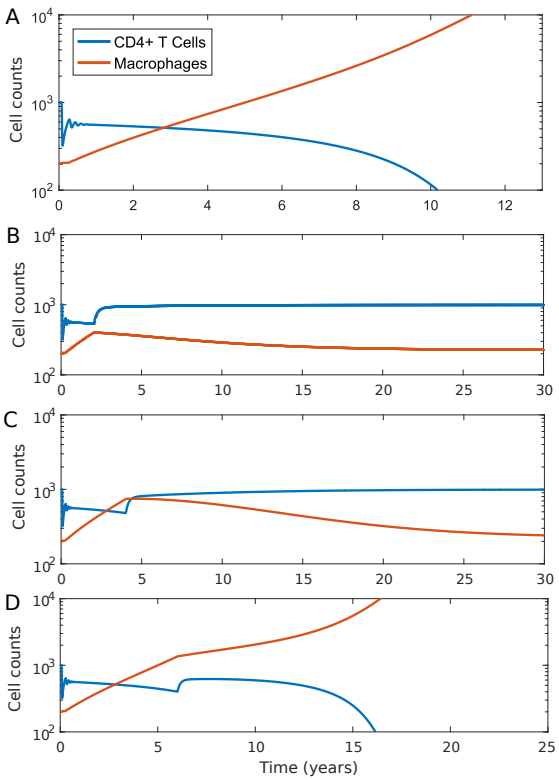

Fig. 4. **PK/PD-based treatment effects on CD4+ T cells and infected macrophages**. A) case without treatment, B-D) depict treatments initiated at 2, 4 and 6 ypi, respectively.

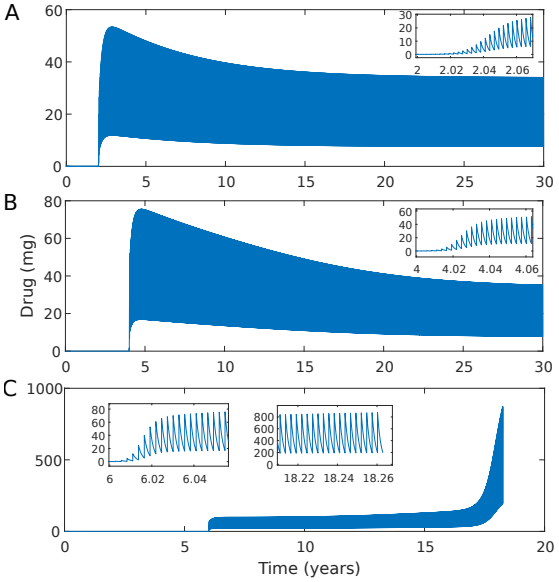

Fig. 5. **Drug amount under PK/PD-based treatment**. A-B) Intake drug amount initiating at 2 and 4 ypi, respectively. C) Intake drug amount initiating at 6 ypi. Zoom windows allow identifying the impulsive drug input from the treatment initiation.

Fig. 3 and Fig. 4 show the viral load behavior under the impulsively controlled PK/PD-based treatment as well as the CD4+ T cells and macrophages dynamics, respectively. In both figures, panel A shows a case without treatment.

While the virus continuously grows without treatment (Fig. 3-A), a complete collapse of T cells counts can be observed about 10 years post-infection (ypi) which coexist with the extensive growth of infected macrophages (Fig. 4-A). Treatments that initiate 2 or 4 ypi (Fig. 3-B,C) manage to maintain the virus under detectable levels for the complete simulation time (30 years), which is related to the elimination of infected macrophages (Fig. 4-B,C). However, the treatment that initiates 6 ypi does not succeed in maintaining the viral load without further grow after 14 ypi (Fig. 3-D), which is mainly due to the high level of infected macrophages when the treatment initiates (Fig. 3-D), as well as the low number of CD4+ T cells at this time point.

Regarding the drug amount and intake dynamics, Fig. 5 portraits the drug dynamics for treatment initiation at 2, 4 and 6 ypi. The inverse optimal controller sets the amount of drug for each intake based on viral dynamics and PK/PD behavior, note that while for the treatment initiated 2 ypi the drug doses reach less than 60 mg, the treatment initiating at 4 ypi reaches almost 80 mg, both in the first years of treatment (Fig. 5-A,B). This shape is mainly because of the low viral load in these cases. When initiating the treatment at 6 ypi (Fig. 5-C), the control-based amount of drug rapidly reaches more than 60 mg and continues to try to eliminate the viral load through high drug dose (almost 800 mg), however, the great number of infected macrophages cooperate to produce higher viral load, which leads to a point of no return in HIV infection.

5. PK/PD-BASED INFLUENZA TREATMENT

5.1 Influenza and drug dynamics

The antiviral action dynamics represent the drug's impulsive change at every treatment intake (schedule), where the change magnitude is given by the control policy. The within-host model for influenza treatment considers the virus (V), the infected cells (I) and uninfected cells (U), the model writes as follows [Hernandez-Mejia et al. (2019)]

$$\dot{V}(t) = p\left(1 - \frac{OC(t)}{OC(t) + EC_{50o}}\right) I(t) - cV(t), \quad (23)$$

$$\dot{U}(t) = -\beta U(t)V(t), \quad (24)$$

$$\dot{I}(t) = \beta U(t)V(t) - \delta I(t), \quad (25)$$

$$\dot{OP}(t) = k_a G(t) - k_f OP(t), \quad (26)$$

$$\dot{OC}(t) = k_f OP(t) - k_e OC(t), \quad (27)$$

$$\dot{G}(t) = -k_a G(t), \ t \neq \tau_j, \ \tau_j \leqslant t < \tau_{j+1} \quad (28)$$

$$G(\tau_j^+) = U_G(\tau_j) + G(\tau_j^-), \ t = \tau_j. \quad (29)$$

Parameter values for equations (23)-(28) are β (0.19×10^{-2} ml/d·TCID$_{50}$), δ (2.6 days^{-1}), p (70×10^{-5} TCID$_{50}$/d·ml) and c (6 days^{-1}). The initial conditions for the influenza system were taken from [Handel et al. (2007)], these are 1×10^{-5} TCID$_{50}$/ml for the virus, the uninfected cells as 4×10^8 cells and zero for infected cells.

The PK oseltamivir model is given by a three-compartment model representing the oseltamivir phosphate (OP), the active metabolic compound form oseltamivir carboxylate (OC), and the depot compartment (G) of dose administered before the adsorption in the blood at rate k_a [Davies (2010)]. The initial values of the drug's depot compartment, as well as $OP(0)$ and $OC(0)$, are zero (mg), changing only when the dose takes place. The parameter values of the drug are k_a (24.24 days^{-1}), k_f (16.41 days^{-1}) and k_e (3.26 days^{-1}). k_a is considered to be reduced with a decay rate of 7.31 after a dose intake [Canini et al. (2014); Wattanagoon et al. (2009)]. On the other hand, the value of the oseltamivir PD phase, EC_{50o}, ranges between 0.0008 to > 35 μM, where 1μM $= 0.284$ μg/mL [La Roche Ltd (2019-Online)]. Based on oseltamivir treatment data, we consider 0.028 μM, comparable to ca. 0.4 mg [Hernandez-Mejia et al. (2019)].

5.2 PK/PD-based influenza treatment

We compare the control-based treatment with the current FDA recommended treatment with doses of 75 mg of oseltamivir at τ_j, with $j = 12\times1, 2, \cdots$, standing for a drug intake each 12 h for 7 days. The control-based treatment considers $u_{max} = 75$ mg and the same impulsive instants τ_j. For the control law (13), the matrix $P_{j(IAV)}$ is as follows

$$P_{j(IAV)} = \begin{bmatrix} 1 & 0 & 0 & 0 & 0 & 0 \\ 0 & 1 & 0 & 0 & 0 & 0 \\ 0 & 0 & 1 & 0 & 0 & 0 \\ 0 & 0 & 0 & 1 & 0 & 0 \\ 0 & 0 & 0 & 0 & 1 & 0.00039 \\ 0 & 0 & 0 & 0 & 0.00039 & 1 \end{bmatrix}.$$

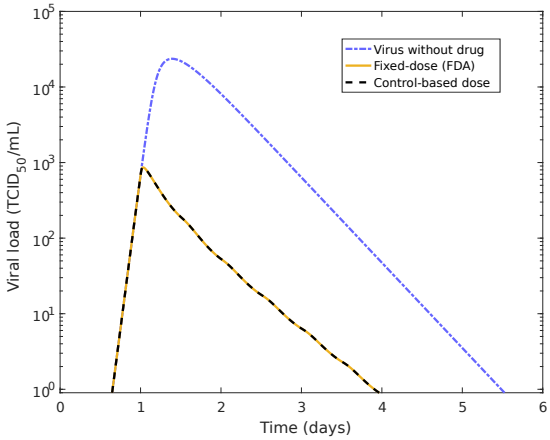

Fig. 6. **Influenza viral load.** The current FDA treatment scheme with fixed-dose in solid line. PK/PD-based treatment in dashed line and viral load without treatment in dash-dotted line.

In addition, we select the order of the state vector as follows $x(t) = [G(t), CO(t), OP(t), U(t), I(t), V(t)]$ and $g(x(\tau_j)) = [0, 0, 0, 0, 0, 1]$ to form matrices $P_\alpha(x(\tau_j))$ and $P_\beta(x(\tau_j))$ of control law (13). We also use the absolute value of the control law and matrix R for positive values of drug amounts. Influenza treatment following FDA and control-based schemes manage to eliminate the viral load after 3 days post-infection (dpi) initiating treatment one dpi, shown in Fig. 6. Importantly, while both schemes equally eliminate the viral load, the PK/PD control-based treatment administered 30% less total drug (630

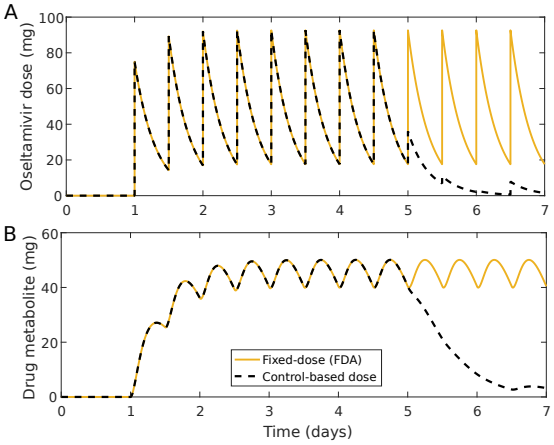

Fig. 7. **Drug dynamics of fixed- and controlled-dose.** A) Dynamics of oseltamivir depot compartment G. B) Dynamics of OC compartment. The control-based dose is considerably reduced as the viral load goes down (Fig. 6).

mg) than the FDA scheme (900 mg). Note that PK/PD-based treatment in Fig. 7 greatly decreases the drug input amounts after 5 dpi. We use the treatment efficacy indicator (E_f) considering the area under the viral curve (VC) without treatment, and the area under the viral curve with treatment (VC_t), that is $E_f = 100(1 - \frac{VC_t}{VC})\%$. Both case treatments reach more than 98% of efficacy.

6. CONCLUSION

We tailor treatment policies for infectious diseases such as HIV and IAV integrating an inverse optimal impulsive control scheme. The controller considers PK/PD and viral dynamics for successful viral mitigation. Further advances in state estimation approaches using neural networks and polynomial models may add to the advantages of experimental outcomes, adding solutions to limitations in the clinical practice.

REFERENCES

Canini, L., Conway, J.M., Perelson, A.S., and Carrat, F. (2014). Impact of different oseltamivir regimens on treating influenza A virus infection and resistance emergence: insights from a modelling study. *PLoS Comput Biol*, 10(4).

Davies, B.E. (2010). Pharmacokinetics of oseltamivir: an oral antiviral for the treatment and prophylaxis of influenza in diverse populations. *Journal of antimicrobial chemotherapy*, 65(suppl 2), ii5–ii10.

Gabrielsson, J. and Weiner, D. (2017). *Pharmacokinetic and pharmacodynamic data analysis: concepts and applications*. CRC Press.

González, A.H., Rivadeneira, P.S., Ferramosca, A., Magdelaine, N., and Moog, C.H. (2017). Impulsive zone MPC for type i diabetic patients based on a long-term model. *IFAC-PapersOnLine*, 50(1), 14729–14734.

Haddad, W.M., Chellaboina, V., and Nersesov, S.G. (2006). *Impulsive and Hybrid Dynamical Systems: Stability, Dissipativity, and Control*. Princeton University Press.

Handel, A., Longini Jr, I.M., and Antia, R. (2007). Neuraminidase inhibitor resistance in influenza: assessing the danger of its generation and spread. *PLoS Computational Biology*, 3(12), e240.

Hernandez-Mejia, G., Alanis, A.Y., Hernandez-Gonzalez, M., Findeisen, R., and Hernandez-Vargas, E.A. (2019). Passivity-based inverse optimal impulsive control for influenza treatment in the host. *IEEE Transactions on Control Systems Technology*.

Hernandez-Mejia, G., Alanis, A.Y., and Hernandez-Vargas, E.A. (2018). Neural inverse optimal control for discrete-time impulsive systems. *Neurocomputing*, 314, 101–108.

Hernandez-Vargas, E.A. (2017). Modeling kick-kill strategies toward HIV cure. *Frontiers in immunology*, 8, 995.

Hernandez-Vargas, E.A. and Middleton, R.H. (2013). Modeling the three stages in HIV infection. *Journal of theoretical biology*, 320, 33–40.

HIV-CC (2010). The effect of combined antiretroviral therapy on the overall mortality of HIV-infected individuals. The HIV-causal-collaboration. *AIDS (London, England)*, 24(1), 123.

La Roche Ltd, S. (2019-Online). Tamiflu (oseltamivir phosphate) capsules and oral suspension. *https://www.accessdata.fda.gov/drugsatfda-docs/nda/2000/21-246-Tamiflu-Prntlbl.pdf*.

Rivadeneira, P.S., Caicedo, M., Ferramosca, A., and González, A.H. (2017). Impulsive zone model predictive control (iZMPC) for therapeutic treatments: application to HIV dynamics. In *2017 IEEE 56th Annual Conference on Decision and Control (CDC)*, 4094–4099. IEEE.

Sanchez, E.N. and Ornelas-Tellez, F. (2017). *Discrete-time inverse optimal control for nonlinear systems*. CRC Press.

Van der Graaf, P.H. and Benson, N. (2011). Systems pharmacology: bridging systems biology and pharmacokinetics-pharmacodynamics (PK-PD) in drug discovery and development. *Pharmaceutical research*, 28(7), 1460–1464.

Wattanagoon, Y., Stepniewska, K., Lindegårdh, N., Pukrittayakamee, S., Silachamroon, U., Piyaphanee, W., Singtoroj, T., Hanpithakpong, W., Davies, G., Tarning, J., et al. (2009). Pharmacokinetics of high-dose oseltamivir in healthy volunteers. *Antimicrobial agents and chemotherapy*, 53(3), 945–952.

WHO (2018-Online). World Health Organization. Influenza (Seasonal) fact sheet. *https://www.who.int/news-room/fact-sheets/detail/influenza-(seasonal)*.

WHO (2019-Online). World Health Organization, Global HIV situation; key facts. *https://www.who.int/news-room/fact-sheets/detail/hiv-aids*.

Yang, T. (2001). *Impulsive control theory*, volume 272. Springer Science & Business Media.

Yu, Y., Rüppel, D., Weber, W., and Derendorf, H. (2019). PK/PD approaches. *Drug Discovery and Evaluation: Methods in Clinical Pharmacology*, 1–23.

Zurakowski, R. and Teel, A.R. (2006). A model predictive control based scheduling method for HIV therapy. *Journal of Theoretical Biology*, 238(2), 368–382.